

Analysis of Leakage Current through Al/HfAlO_x/SiON_x/Si(100) MOS Capacitors

S. Nagamachi, A. Ohta, F. Takeno, H. Nakagawa, H. Murakami,
S. Miyazaki, T. Kawahara* and K. Torii*

Graduate School of AdSM, Hiroshima University, Kagamiyama 1-3-1, Higashi-hiroshima 739-8530, Japan
Fax: 81-082-422-7038, E-mail: semicon@hiroshima-u.ac.jp

*Semiconductor Leading Edge Technologies, Inc., 34-1 Miyukigaoka Tukuba, Ibaraki 305-8501, Japan

We determined the energy band alignment of HfAlO_x/SiON_x stack dielectric and Si(100) and analyzed the leakage current through the Al-gate MIS capacitors with dielectric stack structures by using a multiple-scattering theory which well-reproduces the tunnel current for the case of n⁺ poly-Si/SiO₂/Si(100). HfAlO_x (Hf/(Hf+Al)≈0.3) in the thickness range of 3-7nm were formed on 1.2nm-thick SiON with an N content of ~20at.% prepared on p-Si(100) by an ALCVD method. From the onset of O1s energy loss spectra and the analysis of the valence band spectra, the energy band gap and valence band offset between HfAlO_x and Si(100) were 6.50eV and 3.60eV, respectively. With 3.0nm-thick HfAlO_x, the calculated tunnel current agrees with the measured current if the effective mass of electrons tunneling through HfAlO_x is assumed to be ~0.5m₀. In contrast, with 5.0 and 7.0nm-thick HfAlO_x, the measured leakage current was markedly larger than the calculated tunnel current level. Frenkel-Poole conduction is responsible for this extra leakage current because the current at oxide voltages higher than 1V is proportional to the square root of the oxide field and the permittivity derived from the slope of the Frenkel-Poole plot is almost equal to the value obtained from the accumulation capacitance.

Key words: tunnel current, direct tunneling, energy band alignment

1. INTRODUCTION

The implementation of a gate dielectric with high dielectric constant (high-k) is currently one of major technological challenges for the continuous scaling of complementary metal-oxide-semiconductor (CMOS) devices to sub-100nm technologies [1]. Although the use of a physically thicker high-k gate dielectric for the same electrically equivalent SiO₂ thickness (EOT) is an efficient way to achieve a reduction in the gate leakage to some practical limit under a required capacitive coupling between the gate and Si(100), there are formidable difficulties regarding interface issues and electrically active defects in most high-k dielectrics [2]. With a systematic consideration of the required properties of gate dielectrics such as favorable energy band alignment to Si(100), high thermal stability and process integration compatibility, attention has focused on Hf-silicates and Hf-aluminates as the most promising replacements for conventional SiON gate dielectrics [3, 4]. In fact, a significant reduction of leakage current through Hf-silicate or Hf-aluminate in comparison with SiO₂ has been reported and the scalability to 1nm in EOT has been claimed [3, 4]. However, a quantitative explanation on the leakage current through the gate dielectric or its mechanism was not found. In targeting EOT below 1nm, there are two key issues. First, minimization of the interfacial layer formation between high-k dielectric and Si(100) during the deposition of a high-k dielectric layer and during post-deposition anneal (PDA) in oxidizing ambient, which reduces the leakage current. The physical properties of the interfacial layer have a strong effect on leakage. Second, the replacement for poly Si-base gates with metal gates, which eliminates carrier depletion effect [5] and Fermi level pinning [6] but faces a new set of formidable challenges on manufacturing

and reliability. Because the metal has continues filled electronic states below Fermi level, an increase in the gate leakage is of particular concern compared with poly-Si gate.

In this work, to characterize the leakage current through Al/HfAlO_x/SiON_x/Si(100) stack structures with different HfAlO_x thicknesses, first we determined the energy band alignment of the stack structures by x-ray photoelectron spectroscopy. By applying a multiple-scattering theory, which well-reproduces the tunnel current for the case of n⁺ poly-Si/SiO₂/Si(100) [7], to the energy band profile, we simulated the ideal current-voltage (I-V) characteristics and compared them with the measured results. The conduction mechanism involving traps is also discussed.

2. EXPERIMENTAL

The substrates used in this study were 300mm p-Si(100) wafers. After wet-chemical cleaning, the wafer surface was nitrified at 700°C in pure NH₃ ambient and oxidized in NO, which resulted in a 1.2nm-thick SiON_x layer [8]. Subsequently, HfAlO_x (Hf/(Hf+Al)≈0.3) films in the thickness range of 3 to 7nm were formed on the SiON_x layer by atomic layer controlled chemical-vapor-deposition (ALCVD), where Hf[N(C₂H₅)CH₃]₄, Al(CH₃)₃, and H₂O were used as precursors and remote plasma nitridation using pure NH₃/Ar was performed at each ALCVD cycle. Post deposition anneal at 1000°C for 1 sec in 0.2 % O₂ diluted with N₂ was carried out. The analysis of the stack structure in the thickness direction was made by x-ray photoelectron spectroscopy (XPS) using monochromatized AlKα (1486.6eV) radiation in combination with a wet-chemical etching in a 0.1% HF solution. For MIS capacitors with Al electrodes formed by thermal evaporation, the capacitance-voltage (C-V) and current-voltage (I-V) characteristics were

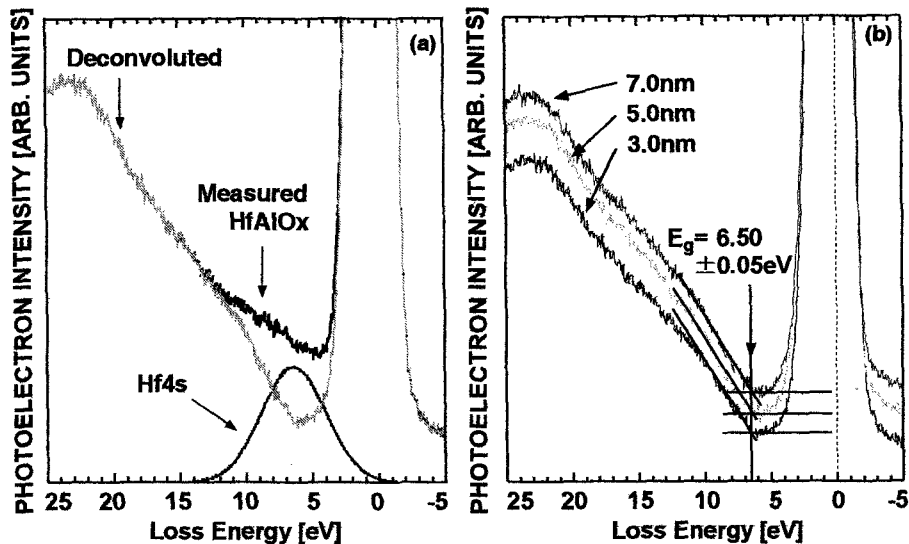


Fig. 1. O1s energy loss spectra for 3.0 nm-thick HfAlO_x (a) and after subtraction of Hf4s contribution from the samples in the thickness range from 3 to 7 nm (b). The measured spectrum for 3.0 nm-thick HfAlO_x was deconvoluted into inherent O1s energy loss signals and Hf4s signals in (a). The onset of the energy loss signals for each sample was determined with an accuracy of ± 0.05 eV.

measured at room temperature.

3. RESULTS AND DISCUSSION

No indication of crystallization was detected by transmission electron microscope (TEM) observations. Atomic force microscope (AFM) images confirmed a very smooth dielectric surface after PDA and a fairly uniform thinning of the dielectrics in the dilute HF-etching. The depth analysis of Si2p, N1s, O1s and Hf4f spectra showed a slight compositional intermixing in the dielectric stack. A few at.% of Si atoms were incorporated in HfAlO_x. The N content was ~ 1 at.% in HfAlO_x and ~ 20 at.% in SiON_x. To evaluate the energy bandgap of the HfAlO_x films, the energy loss signals of O1s photoelectrons from the HfAlO_x layers were measured as shown in Fig. 1. Considering the fact that Hf4s signals overlap with the energy loss spectrum of the primary O1s core line signals [9], we first subtracted the Hf4s component expected from Hf4f signal intensity from the measured spectrum to obtain an inherent background of the O1s core line signals and then defined the onset with a linear extrapolation of a leading segment to the background level. The energy bandgap of HfAlO_x film was determined to be constant at 6.50 eV within an accuracy of 100 meV, regardless of the HfAlO_x thickness (Fig. 1 (b)). As for the energy band gap of the interfacial SiON_x layer, the O1s energy loss spectrum was taken after complete removal of the top HfAlO_x layer by dilute HF etching and compared to the spectrum for 1.6 nm-thick thermally grown SiO₂ on Si(100) as represented in Fig. 2. Although a similarity in the spectral structure between the two cases was observable, the energy loss signals for the SiON_x showed some remarkable tailing and the onset energy (7.5 eV) was significantly shifted toward the lower energy side compared with that (8.95 eV) for the SiO₂ case determined by line-fitting in the same energy region. The N2p non-bonding states are thought to be responsible for the measured bandgap shrinkage and band tailing. To determine the valence band offset

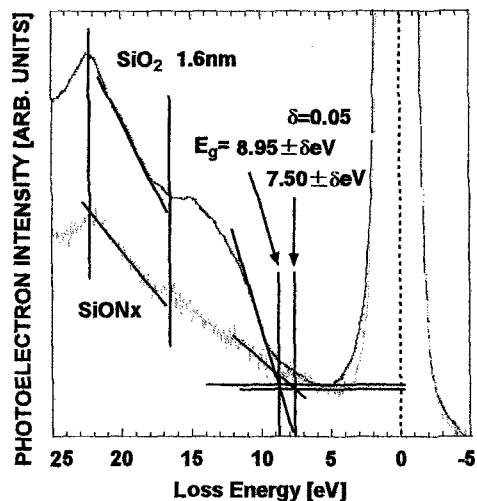


Fig. 2. O1s energy loss spectra for SiON_x/Si(100) after complete removal of the top HfAlO_x layer and for 1.6 nm-thick thermally-grown SiO₂.

(VBO) between HfAlO_x and Si(100), the valence band spectra for HfAlO_x/SiON_x stack structures on Si(100) were measured and first deconvoluted into two components as shown in Fig. 3. In the spectral deconvolution, the valence band spectrum measured after complete removal of the top HfAlO_x layer, that is SiON_x/Si(100) as shown in Fig. 2, was used and the binding energy for each valence band spectrum was calibrated with the Si2p(3/2) core line peak due to the Si(100) substrate. From the energy separation of the tops of the deconvoluted valence band spectra, the VBO between HfAlO_x and Si(100) was determined to be 3.6 eV (Fig. 3). The result indicates that the conduction band offset (CBO) between HfAlO_x and Si(100) is 1.78 eV in consideration of the energy bandgap. From further spectral deconvolution of the valence band spectrum of SiON_x/Si(100) by using the

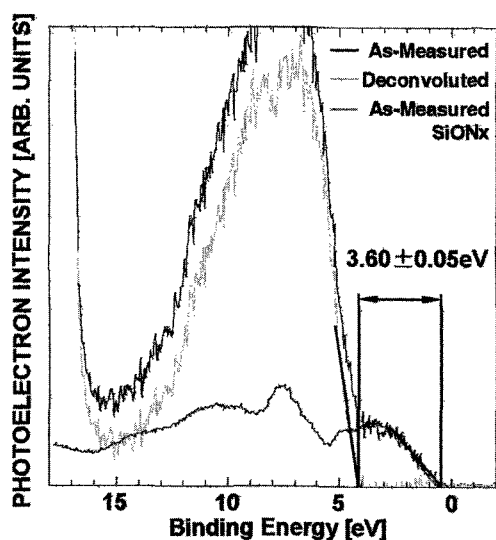


Fig. 3. Valence band spectrum for 3.0 nm-thick $\text{HfAlO}_x/\text{SiON}_x/\text{Si}(100)$ and spectral deconvolution using the spectrum measured for $\text{SiON}_x/\text{Si}(100)$ after complete HfAlO_x removal with the consideration of the binding energy of the $\text{Si}2p$ core line peak. By the spectral deconvolution, the HfAlO_x component (deconvoluted) was extracted from the measured spectrum of the stack structure.

spectrum separately measured for H-terminated $\text{Si}(100)$, the spectrum due to the SiON_x valence band is extracted and very similar to the valence band spectrum for thermally grown SiO_2 as shown in Fig. 4. Obviously, two threshold energies can be determined near the low energy edge of the SiON_x valence band spectrum. The lower threshold ($\sim 3.2\text{eV}$ from the Si valence band top) is attributable to the band edge for the nitrogen-rich region and the higher one ($\sim 4.5\text{eV}$ from the Si valence band top) is identical to the band edge for the SiO_2 network. Thus, the CBO between the SiON_x interfacial and $\text{Si}(100)$ is estimated to be 3.18eV for $\text{VBO} = 3.2\text{eV}$ or 3.33eV for $\text{VBO} = 4.5\text{eV}$ (Fig. 5), being almost equal to the value for thermally grown $\text{SiO}_2/\text{Si}(100)$ interface [10].

High-frequency capacitance-voltage (C-V) characteristics of Al-gate MIS capacitors with different HfAlO_x thicknesses were evaluated by a two-frequency C-V method [11] and, from the plot of the reciprocal values of accumulation capacitances as a function of the HfAlO_x thickness, the dielectric constants of HfAlO_x and SiON_x were estimated to be $12.8\epsilon_0$ and $4.1\epsilon_0$, respectively, where ϵ_0 is permeability in the vacuum. From the measured flat-band voltage shift, net positive fixed charge densities for 3nm-thick and 7nm-thick HfAlO_x cases were obtained to be 3.8×10^{12} and $1.5 \times 10^{12} \text{ cm}^{-2}$, respectively. A C-V hysteresis in the range of 30-40mV due to the electron injection into oxide traps was also measured. Figure 6 shows I-V characteristics for Al-gate MIS capacitors measured with negative gate biases, in which the voltage through the dielectric stack was determined from the C-V characteristics, and compared with simulated results for tunnel currents through the stack structures from the Al gate. In the simulation, a multiple-scattering theory [12] was applied to the measured energy band profile. The effective mass of electrons

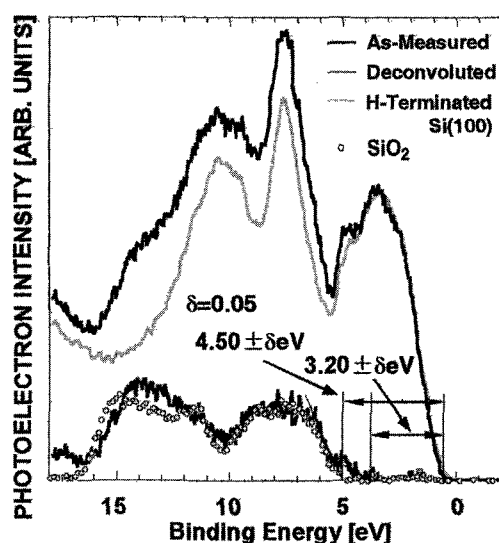


Fig. 4. Valence band spectrum for the $\text{SiON}_x/\text{Si}(100)$ shown in Fig. 3 and spectral deconvolution using the spectrum for wet-chemically prepared H-terminated $\text{Si}(100)$ with consideration of the binding energy of the $\text{Si}2p$ core line peak. By the spectral deconvolution, the SiON_x component (deconvoluted) was extracted and compared with the reference valence-band spectrum of thermally grown SiO_2 (open circles).

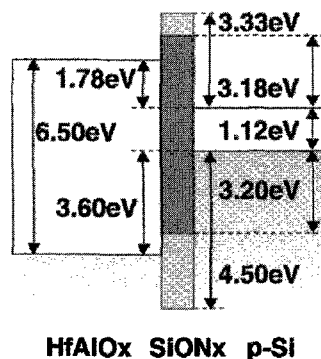


Fig. 5. Energy band alignment of HfAlO_x ($\text{Hf}/(\text{Hf}+\text{Al}) = \sim 0.3$) to $\text{Si}(100)$, including interfacial SiON_x .

tunneling through SiON_x was set to be $0.35m_0$, where m_0 is the free electron mass. The effective mass of electrons tunneling through HfAlO_x was set at $0.50m_0$ for the case of 3.33eV in CBO between SiON_x and $\text{Si}(100)$ and at $0.51m_0$ for the case of 3.18eV in CBO between SiON_x and $\text{Si}(100)$. For the case with 3.0nm-thick HfAlO_x , the measured leakage current at oxide voltages higher than 0.5V is well reproduced with the tunnel current calculation mentioned above. A significantly enhanced leakage current at voltages below 0.5V in comparison to the simulated result suggests that trap-assisted tunneling is dominant in the low electric-field. In contrast, for the cases with 5.0nm-thick and 7.0nm-thick HfAlO_x , the measured leakage current is markedly larger than the calculated tunnel current level. The plot of the leakage current vs. the square root of the oxide field indicates the field-enhanced thermal emission of trapped electrons, or so-called "Frenkel-Poole emission", becomes significant at oxide voltages

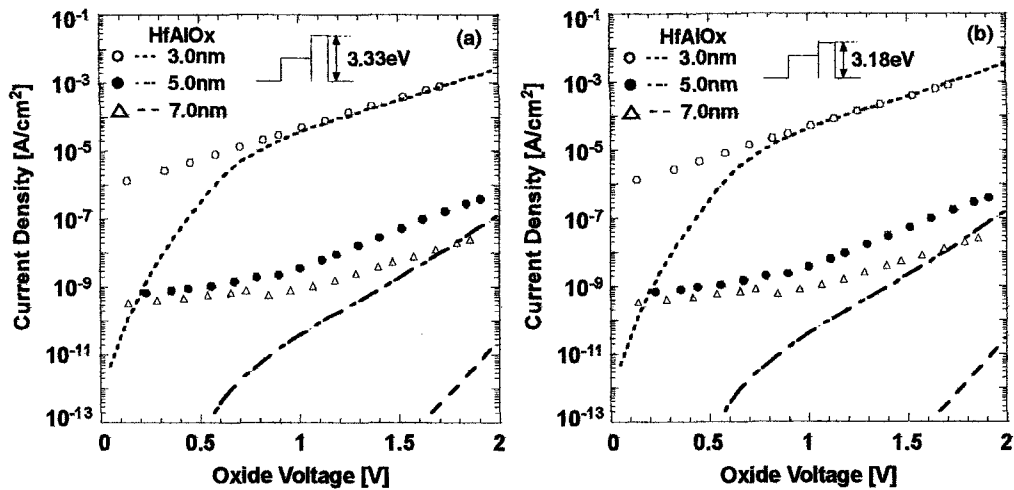


Fig. 6. The measured leakage currents (symbols) for Al-gate MIS capacitors with different HfAlO_x thickness as a function of the oxide field in negative gate bias and comparison to the simulated I-V curves (lines) for the stack structures with an energy band profile shown in Fig. 5 using a multiple-scattering theory[12]. The simulated results are shown for each case with a conduction band offset between interfacial SiON_x and Si(100) of 3.33eV (a) or 3.18eV (b), where the effective mass of tunneling electrons was set to be 0.5m₀ (a) or 0.51m₀ (b).

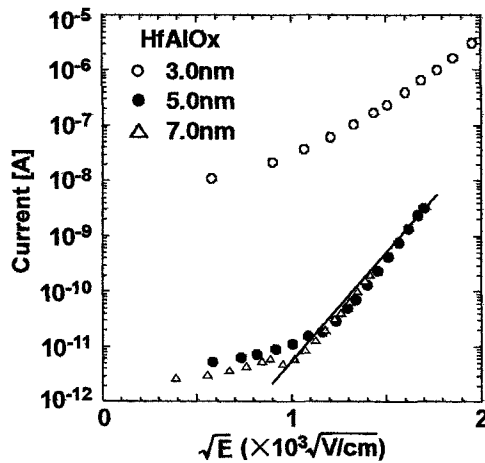


Fig. 7. The plots of measured leakage currents shown in Fig. 6 vs. the square root of the electric field in HfAlO_x.

higher than ~1V because the dielectric constant estimated from the slope of the Frenkel-Poole plot in the high electric field region is ~10ε₀ and fairly close to the value (12.8ε₀) obtained from the C-V measurements as described above.

4. CONCLUSIONS

The energy band alignment of the stack structure consisting of HfAlO_x (Hf/(Hf+Al)~0.3) and an interfacial SiON_x layer with respect to Si(100) was determined by the analyses of O1s energy loss spectrum and valence band spectrum. By applying a multiple-scattering theory for electron tunneling through a dielectric stack structure to the experimentally determined energy band profile, the intrinsic leakage due to electron tunneling from Al-gate to Si(100) substrate with any assistance of traps was calculated and compared with the measured leakage current of Al-gate MIS capacitors with different HfAlO_x thicknesses. The leakage current of the case with 3nm-thick HfAlO_x is interpreted in terms of direct tunneling at oxide voltages higher than 1V and trap-assisted tunneling below 1V. The

effective mass of tunneling electrons through HfAlO_x was estimated to be ~0.5m₀. For HfAlO_x thicker than 5nm, the enhanced leakage current in the oxide field higher than ~2MV/cm is attributed to Frenkel-Poole emission.

ACKNOWLEDGEMENTS

The authors wish to thank the members of the research project "High-k Network" for their fruitful comments and discussion.

REFERENCES

- [1] "High Dielectric Constant Materials", Eds H. R. Huff and D. C. Gilmer (2004, Springer).
- [2] G. D. Wilk, R. M. Wallace and J. M. Anthony: J. Appl. Phys. 89 (2001) 5243.
- [3] G. D. Wilk, R. M. Wallace and J. M. Anthony: J. Appl. Phys. 87 (2000) 484.
- [4] A. Muto, H. Ohji, T. Kawahara, T. Maeda, K. Torii and H. Kitajima: Extend Abst. of International Workshop on Gate Insulator (Tokyo, 2003) p. 64.
- [5] W-C. Lee, B. Watson, T-J. King and C. Hu: IEEE Electron Dev. Lett. 20(5) (1999) 232.
- [6] C. W. Yang, Y. K. Fang, C. H. Chen, S. F. Chen, C. Y. Lin, C. S. Lin, M. F. Lin, T. H. Hou, C. H. Chen, L. G. Yao, S. C. Chen and M. S. Liang: Appl. Phys. Lett. Vol.83 (2003) 308.
- [7] M. Fukuda, W. Mizubayashi, A. Kohno, S. Miyazaki and M. Hirose: Jpn. J. Appl. Phys. 37 (1998) L1534.
- [8] R. Mitsuhashi, K. Torii, H. Ohji, T. Kawahara, A. Horiuchi, H. Takada, M. Takahashi and H. Kitajima: Extend Abst. of the Intern. Conf. on Solid State Devices and Materials (Tokyo, 2004) 34.
- [9] M. Yamaoka, M. Narasaki, H. Murakami and S. Miyazaki: Proc. of ECS Int. Semicond. Technol. Conf. (2002, Tokyo) 229.
- [10] S. Miyazaki, H. Nishimura, M. Fukuda, L. Ley, and J. Ristein: Appl. Surf. Sci. 113/114 (1997) 585-589.
- [11] K. J. Yang and C. Hu: IEEE Trans. Electron Devices 46 (1999) 1500.
- [12] T. M. Kalotas and A. R. Lee: Am. J. Phys. 59 (1991) 48.